

COMPRESSIVE SENSING FOR HIGH RESOLUTION DIFFERENTIAL SAR TOMOGRAPHY

Xiao Xiang Zhu¹, Richard Bamler^{1,2}

¹Technische Universität München, Lehrstuhl für Methodik der Fernerkundung, Arcisstraße 21, 80333, München, Germany. Contact: xiao.zhu@dlr.de

²German Aerospace Center (DLR), Remote Sensing Technology Institute (IMF), Germany

ABSTRACT

Differential SAR tomography extends the synthetic aperture principle into the elevation and time directions for 4-D imaging. With modern meter-resolution space-borne SAR systems like TerraSAR-X and COSMO-SkyMed systematic tomographic imaging of urban infrastructure and its deformations becomes feasible. We demonstrate the use of TerraSAR-X data for this purpose and introduce several novel concepts.

Since building deformation in general is nonlinear, e.g. due to thermal dilation, we start from a tomographic system formulation that is general enough to allow for the inclusion of motion models (linear, periodic, etc.). By appropriate warping of the time axis we map the motion model function to become linear and lead to a peak in the spectral domain.

For the differential tomographic inversion itself we propose a 2-D compressive sensing (CS) approach. CS requires sparsity of the signals to be reconstructed which is true for meter-resolution SAR data of urban environment. We demonstrate the super-resolution power and the robustness of CS both with simulated and with real data. We also show that CS is an attractive compromise between parametric and non-parametric methods. A full reconstruction of a building complex and its seasonal deformation from a stack of TerraSAR-X spotlight data is finally presented.

Index Terms— differential SAR tomography, nonlinear motion, compressive sensing, super-resolution

1. INTRODUCTION

Differential SAR Tomography (D-TomoSAR), also referred to as 4-D focusing, uses stacks of repeat-pass acquisitions to reconstruct reflectivity and deformation profiles of the scattering objects along elevation s by means of 2-D spectral analysis for every azimuth-range (x - r) pixel.

Currently, very high spatial resolution (VHR) SAR satellites like TerraSAR-X (TS-X) and COSMO-SkyMed provide data up to 1m resolution, which are particularly suited for tomographic imaging of urban infrastructure and their temporal deformations. Due to the repeat-pass nature of data acquisition, deformation terms must always be accounted for by the reconstruction algorithms, and be it only as nuisance parameters. Most often pronounced seasonal thermal dilation prohibits the use of the popular linear motion assumption. In this paper we propose a model-based time warp method for nonlinear motion monitoring.

Due to the tight orbit control of these satellites the elevation resolution can be about 50 times (TS-X) worse than the one in azimuth or range. This extreme anisotropy calls for super-resolution algorithms. We work with TS-X spotlight data and concentrate on *single-look* super-resolution methods to exploit the potential of VHR data. All methods that require multi-look estimates of covariance matrices (e.g. CAPON, MUSIC) would reduce the azimuth-range resolution and are not able to resolve structural building elements in the important meter scale. In this paper compressive sensing (CS) [1] D-TomoSAR is introduced and we demonstrate its favourable properties like super-resolution, robustness against phase noise, etc.

2. SYSTEM MODEL

The measurement g_n at an (x - r) pixel for the n th acquisition at aperture position b_n and time t_n ($n = 1, \dots, N$) is [2]:

$$g_n = \int_{\Delta s} \gamma(s) \exp\left(-j2\pi\left(\xi_n s + 2d(s, t_n) / \lambda\right)\right) ds \quad (1)$$

where $\gamma(s)$ represents the reflectivity function along elevation s with an extent of Δs and $\xi_n = -2b_n / (\lambda r)$ is the spatial (elevation) frequency. $d(s, t_n)$ is the line-of-sight (LOS) deformation as a function of elevation and time. By introducing the temporal frequency $\eta_n = 2\tau_n / \lambda$ as a function of an *artificial temporal baseline* τ_n and a *motion parameter* $p(s)$, the proposed time warp method leads to a generalized system model which is adapted for different nonlinear motion models:

$$g_n = \int_{\Delta s} \gamma(s) \exp\left(-j2\pi\left(\xi_n s + \eta_n p(s)\right)\right) ds \quad (2)$$

For instance, in case of *linear* motion, $\tau_n = t_n$ and the motion parameter $p(s)$ stands for the LOS velocity. In case of seasonal motion caused by thermal expansion, $\tau_n = \sin(2\pi(t_n - t_0))$ and the deformation parameter $p(s)$ stands for the amplitude of the periodic motion along s ; t_0 is the initial phase offset which can be estimated from the temperature history. After the time warp, the system model (2) can be easily rewritten as:

$$\mathbf{g}_n = \int \int_{\Delta s \Delta p} a_\gamma(s, p) \exp(-j2\pi(\xi_n s + \eta_n p)) ds dp \quad (3)$$

where $a_\gamma(s, p) = \gamma(s) \delta(p - p(s))$ is the scattering distribution in the elevation-motion (s - p) plane. Equation (3) is a 2-D Fourier transform of $a_\gamma(s, p)$ which is a delta-line in the elevation-motion (s - p) plane along $p = p(s)$. Its projection onto the elevation axis is the reflectivity profile $\gamma(s)$. This model is a generalization of the one introduced in [2]. For the following we use a discretized version of equation (3), i.e. a 2-D discrete Fourier transform:

$$\mathbf{g} = \mathbf{R}\boldsymbol{\gamma} \quad (4)$$

where \mathbf{g} is the measurement vector with N elements, \mathbf{R} with $R_{n \times (l+Lq)} = \exp(-j2\pi(\xi_n s_l + \eta_n p_q))$ is an $N \times LQ$ mapping matrix, $\boldsymbol{\gamma}$ is the discrete $a_\gamma(s, p)$ in elevation s_l ($l=1, \dots, L$) and velocity p_q ($q=1, \dots, Q$). Its inversion provides retrieval of the elevation and deformation information even in the case of multiple scatterers inside an azimuth-range resolution cell.

3. D-TOMOSAR VIA COMPRESSIVE SENSING

Compressive sensing (CS) is a favourable approach for sparse signal reconstruction [1]. As described in [3], for VHR space-borne X-band TomoSAR the signal $\boldsymbol{\gamma}$ to be reconstructed has typically $K=1-3$ point-like contributions of unknown positions, amplitudes, phases, and motion parameters, i.e. $\boldsymbol{\gamma}$ is *sparse* in the identity orthogonal basis \mathbf{I} . In order to measure $\boldsymbol{\gamma}$ efficiently, the sensing matrix \mathbf{R} should spread out the information of localized sparse signals in the entire projection space and thus makes them insensitive to “undersampling”. This property is the so called incoherence between the sensing matrix and the orthogonal basis. According to equations (1) and (2) the sensing matrix \mathbf{R} is a randomly distributed Fourier sampling matrix which is known to have the best incoherence property with \mathbf{I} . The aim is to find the solution of $\boldsymbol{\gamma}$ with least number of scatterers, i.e. minimal L_0 norm, to satisfy measurements:

$$\min_{\boldsymbol{\gamma}} \|\boldsymbol{\gamma}\|_0 \quad \text{s.t.} \quad \mathbf{g} = \mathbf{R}\boldsymbol{\gamma} \quad (5)$$

For $N \geq O(K \log(L/K))$, which is fulfilled due to the small number K of scatterers, CS theory tells us that L_1 norm minimization leads to the same result as L_0 norm. In the presence of noise, the solution can finally be approximated by [4]:

$$\hat{\boldsymbol{\gamma}} = \arg \min_{\boldsymbol{\gamma}} \left\{ \|\mathbf{h} - \mathbf{R}\boldsymbol{\gamma}\|_2^2 + \lambda_K \|\boldsymbol{\gamma}\|_1 \right\} \quad (6)$$

λ_K is a factor adjusted according to the noise level. The choice of λ_K is described in [4]. Equation (6) can be solved by basis pursuit methods [4]. Instead of detecting the K most significant coefficients, they minimize the residual by employing a L_1 norm regularization. By providing the over-completeness of $\boldsymbol{\gamma}$, they provide more robust solutions than (5).

4. EXPERIMENTS

4.1. The Data Set

We work with TS-X spotlight data with a resolution of 0.6m in slant range and 1m in azimuth. Our test site is Las Vegas, Nevada, USA. The orbit of TS-X is controlled in a tube of 500m diameter. The data stack consists of 25 scenes with an elevation aperture size $\Delta b = 269.5$ m. With non-parametric linear spectral analysis based on regularized SVD [2][5] we obtain a 3dB elevation resolution of $\rho_s = 33$ m or about 16m in height z (look angle = 31.8°). The Cramér-Rao lower bound (CRLB) of the elevation estimates of a single scatterer is 1.1m for a SNR=10dB in this configuration [5].

4.2 Simulation

In this section, the CS approach is compared to conventional non-parametric and parametric methods using simulated data with the elevation sampling of the real data. Decorrelation is introduced by adding Gaussian noise with variable SNR. Phase noise due to unmodeled motion and atmospheric effects is simulated by adding a uniformly distributed phase.

Figure 1 shows the 4-D reconstruction with *linear* motion using a singular value decomposition method with Wiener-type regularization (SVD-Wiener) [5] (left) and CS (right). We simulate the situation of two scatterers inside one resolution cell with elevation of 0m and 20m and linear deformation velocity of 0.9 cm/y and 1.1 cm/y, respectively. SVD-Wiener is not able to distinguish them while CS detects very clearly two individual scatterers. Figure 2 shows the same plot as Figure 1 but

with *seasonal* motion. The two scatterers are far apart from each other with elevation of -30 and 20m and seasonal motion amplitude of 8mm and 4mm. With time warp, the amplitudes of seasonal motion can be well reconstructed.

In [3], CS has been compared to maxima detection (MD) and NLS, where MD simply uses the maxima of the SVD-Wiener reconstruction as estimates and NLS is the theoretically best solution under Gaussian noise. Compared to MD, besides the super-resolution property, CS shows no sidelobe interference. Compared to NLS, CS has comparable performance with lower computational effort and does not require the number of scatterers as a prior.

Figure 3 shows the elevation estimation accuracy of a single scatterer in the phase-noise-free case using NLS and CS compared to the CRLB as a function of SNR. The estimation accuracy of CS is almost identical to NLS and reaches the CRLB. Figure 4 shows the elevation error under phase noise uniformly distributed in $[-\phi_n, \phi_n]$. Obviously CS is more robust against non-Gaussian phase noise than NLS. Taking all those aspects into account, CS provides the best of the two worlds of non-parametric and parametric spectral estimation methods and, hence, is proven very attractive for D-TomoSAR.

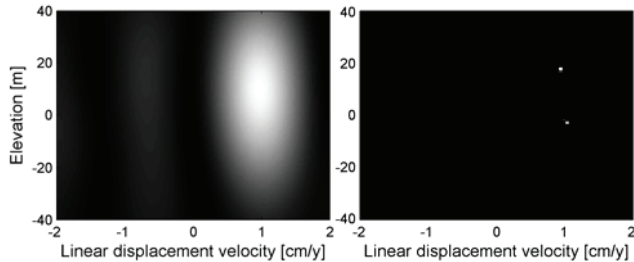


Figure 1: 4-D reconstruction with linear motion: SVD-Wiener (left) vs. CS (right). SNR=10dB; $s=0, 20\text{m}$; $v=0.9\text{cm/y}, 1.1\text{cm/y}$.

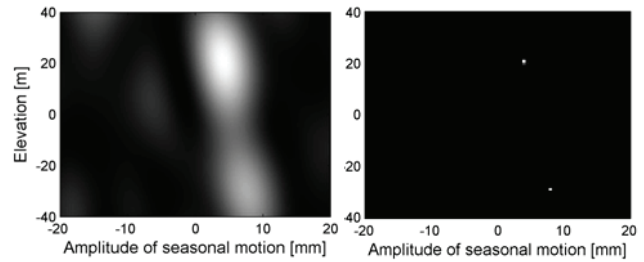


Figure 2: 4-D reconstruction with seasonal motion: SVD-Wiener (left) vs. CS (right). SNR=10dB; $s=-30\text{m}, 20\text{m}$; amplitude of seasonal motion=8mm, 4mm.

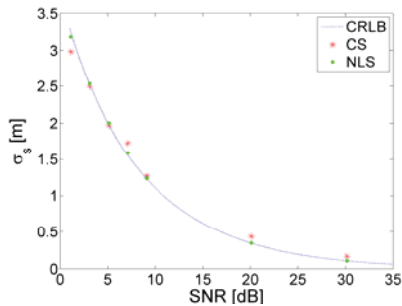


Figure 3: Single scatterer elevation estimation error of NLS and CS compared to the CRLB as a function of SNR

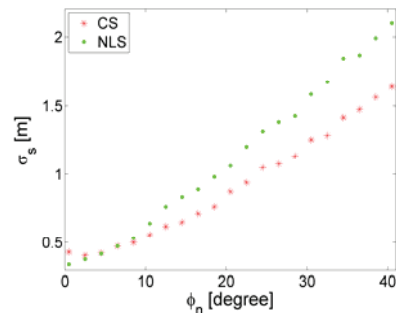


Figure 4: Single scatterer elevation estimation error of NLS and CS as a function of phase noise (SNR=20dB).

4.3 Real Data

We use the Las Vegas convention center as a test site. It has a height of about 20m, roughly the resolution limit of SVD-Wiener for our elevation aperture size. The left image in Figure 5 shows the TS-X intensity map. The presence of two scatterers within an azimuth-range pixel is expected in layover areas and has been validated in [5]. Thus, we are able to compare the performance of CS to SVD-Wiener in the layover areas. Figure 5, center, shows the projections of the 4-D reconstruction for the pixel P (red dot) to elevation direction, i.e. the reflectivity profile. Two scatterers have been detected by SVD-Wiener (red line), one on the roof, the other on the parking place on the ground. The blue line in Figure 5 shows the result using CS. Two very close scatterers have been detected, i.e. D-TomoSAR via CS provides super resolution up to 2m in height (i.e. about 4m in elevation) in this case.

With the approximately one year time spread of our data set, nonlinear (e.g. thermally induced) movements of different building parts must be expected. Hence, by using our time warp method, the surface model and amplitude map of seasonal motion is obtained for the whole building. The center image of Figure 6 shows the surface model generated from the elevation estimates (converted to height). The full structure of the convention center has been captured at a very detailed level. Besides the building, more detail such as the roads surrounding the convention center, as well as two bridges above the roads which have weak but correlated returns are clearly resolved. The height estimates are very precise compared to the 33m elevation resolution due to the high SNR of TS-X data. The right image of Figure 6 represents the amplitude map of the seasonal motion. The amplitude variance is smooth for individual structural blocks with sudden amplitude changes between adjacent blocks. The amplitude difference is up to 8mm. Figure 7 shows the final surface model over-layed with the reflectivity map, i.e. a 3-D SAR image. This visualizes in detail how the convention center would look like from the position of TS-X if our eyes could see X-band radiation. This may lead to a better understanding of the nature of scattering.

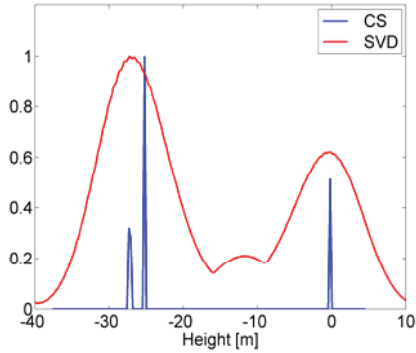


Figure 5: Reflectivity reconstruction for a pixel located at the layover area by using SVD-Wiener (red) and CS (blue).

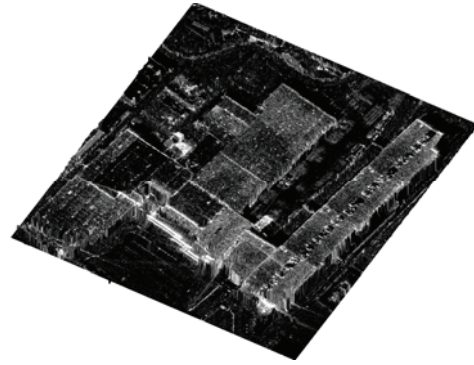


Figure 6: The world at X-band: tomographic surface reconstruction overlaid by 3-D reflectivity map.

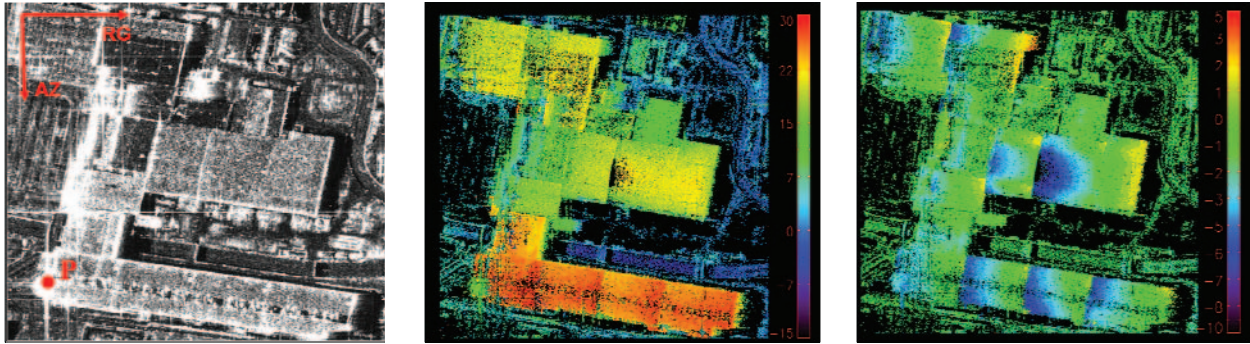


Figure 7: Left: TS-X intensity map of Las Vegas convention center; middle: Reconstructed digital surface model (DSM) from D-TomoSAR, [unit: m]; right: Estimated amplitude of seasonal motion using the time warp method [unit: mm]

5. CONCLUSION

The new class of space-borne high resolution spotlight SAR data is very attractive for 3-D and 4-D tomographic mapping of urban infrastructure. Compared to the medium resolution SAR systems available so far, the information content and level of detail has increased dramatically.

Recognizing the sparsity of the signal in elevation, CS as a new and promising technique for sparse signal reconstruction has been introduced to D-TomoSAR. It provides a very elegant compromise between conventional non-parametric and parametric tomographic methods. For instance, it shows high robustness w.r.t. unmodeled non-Gaussian phase noise. Compared to non-parametric methods, it provides super-resolution properties without sacrificing the azimuth or range resolution; it does not suffer from the sidelobe interference effect. Compared to parametric methods, like NLS, in the single scatterer case and under Gaussian noise CS approaches the accuracy of NLS with lower computational effort. In addition, CS does not need model selection, i.e. it “automatically” chooses the number of scatterers that can be resolved.

A new model-based time warp method has been proposed for nonlinear motion monitoring. By forming an artificial temporal baseline, it provides the possibility of focusing the desired parameter, e.g. the amplitude of seasonal motion, to the coefficient space. The time warp method has been validated by reconstructing seasonal motion caused by thermal expansion of a building complex. A full tomographic high resolution reconstruction of the Las Vegas convention center is presented.

REFERENCES

- [1] E. Candès, *Compressive sampling*, Int. Congress of Mathematics, 3, pp. 1433-1452, Madrid, 2006
- [2] G. Fornaro, D. Reale, F. Serafino, *Four-Dimensional SAR Imaging for Height Estimation and Monitoring of Single and Double Scatterers*, IEEE Trans. Geosci. Remote Sensing, Vol. 47, pp: 224 – 237, 2009
- [3] X. Zhu, R. Bamler, *Tomographic SAR Inversion by L1 Norm Regularization – The Compressive Sensing Approach*, IEEE Transactions on Geoscience and Remote Sensing, submitted.
- [4] S. Chen, D. Donoho, M. Saunders, *Atomic Decomposition by Basis Pursuit*, SIAM Journal on Scientific Computing, Vol. 20, pp.33-61,1998
- [5] X. Zhu, R. Bamler, *Very High Resolution Spaceborne SAR Tomography in Urban Environment*, IEEE Transactions on Geoscience and Remote Sensing, submitted.